Supporting information

Dual-functional coordination polymers with high proton conduction behavior and good luminescence properties

Xue-Ting Liu,[a] Bin-Cheng Wang,[a] Biao-Biao Hao,[a] Chen-Xi Zhang*[a,b] and Qing-Lun Wang[c,d]

[a] College of Chemical Engineering and Materials Science, Tianjin University of Science and Technology, Tianjin 300457, P. R. China

[b] Key Laboratory of Brine Chemical Engineering and Resource Eco-utilization, Tianjin University of Science and Technology, Tianjin 300457, P. R. China

[c] College of Chemistry, Nankai University, Tianjin 300071, P. R. China.

[d] Key Laboratory of Advanced Energy Materials Chemistry (Ministry of Education), Nankai University, Tianjin 300071, P. R. China

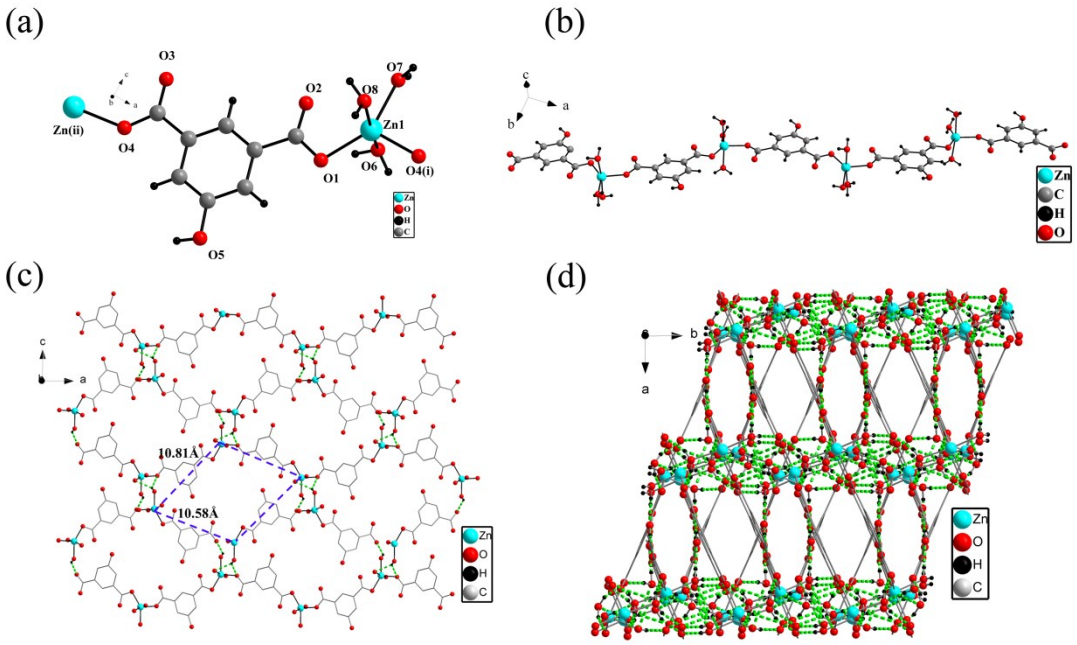

Figure S1 (a) The ligand environment of complex **2**(Symmetry codes: (i) 0.5+x, -0.5+y, 1-z; (ii) -0.5+x, 0.5+y, 1-z**)**, (b) 1D chain structure of complex **2**; (c) 2D planar structure of complex **2**; (b) 3D stacking diagram of complex **2** connected by hydrogen bonds.

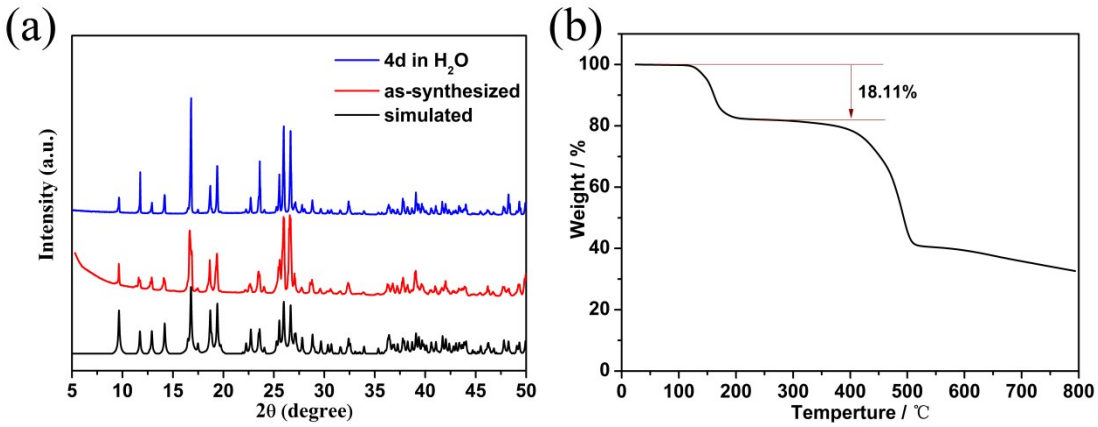

Figure S2 (a) PXRD patterns of complex **2** for the simulated, as-synthesized and after water treated samples; (b) TG analysis profile of complex **2**.

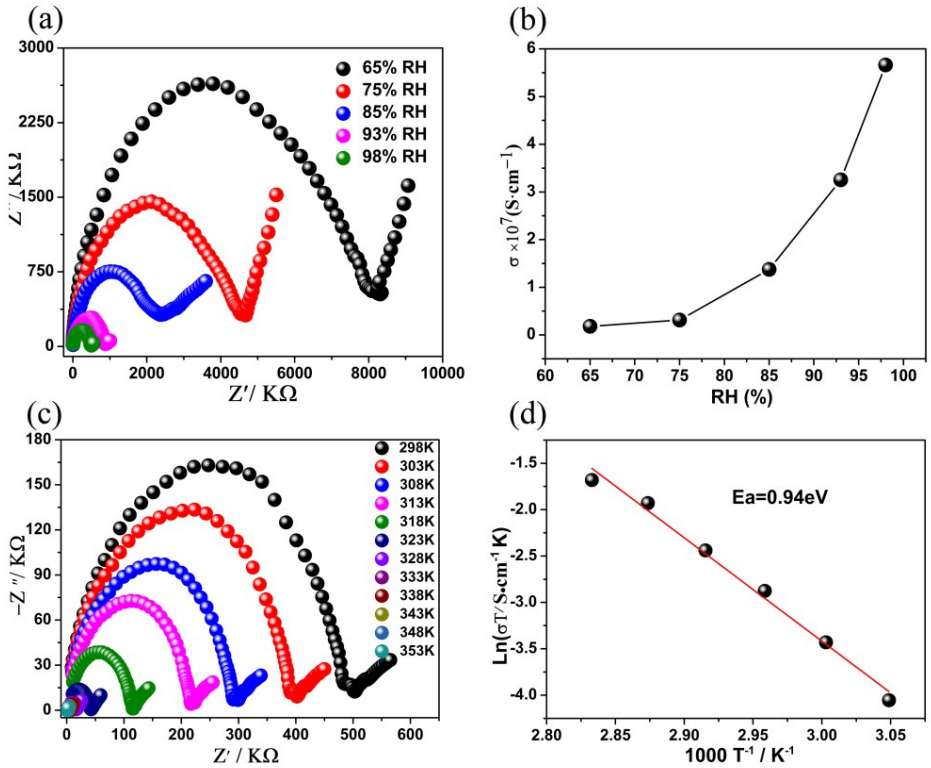

Figure S3 (a) Impedance spectra of complex **2** at 298 K under different humidity; (b) The variation trend of proton conductivity of complex **2** with humidity at 298 K; (c) Impedance spectra of complex **2** at different temperature under 98% RH; (d) Arrhenius plot for activation energy of complex **2** at 98% RH.

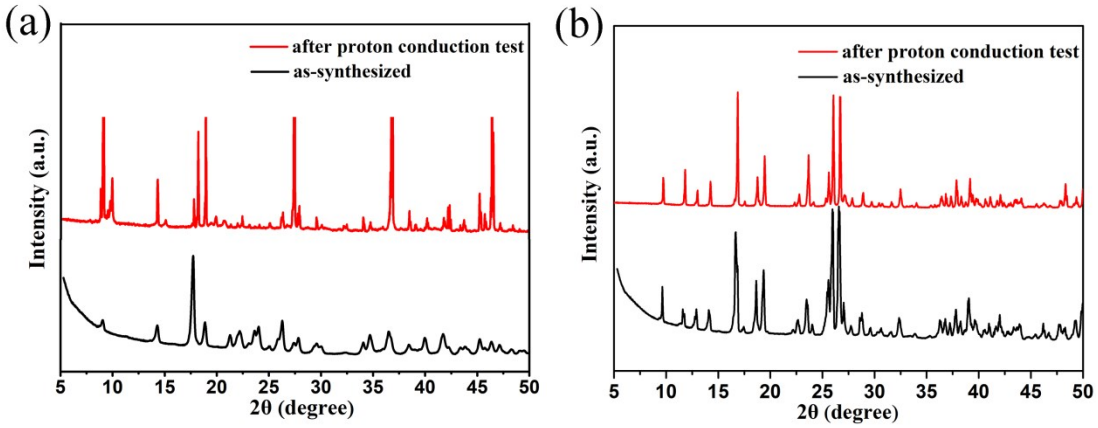

Figure S4 (a) PXRD after proton conduction test of complex **1**; (b) PXRD after proton conduction test of complex **2**.

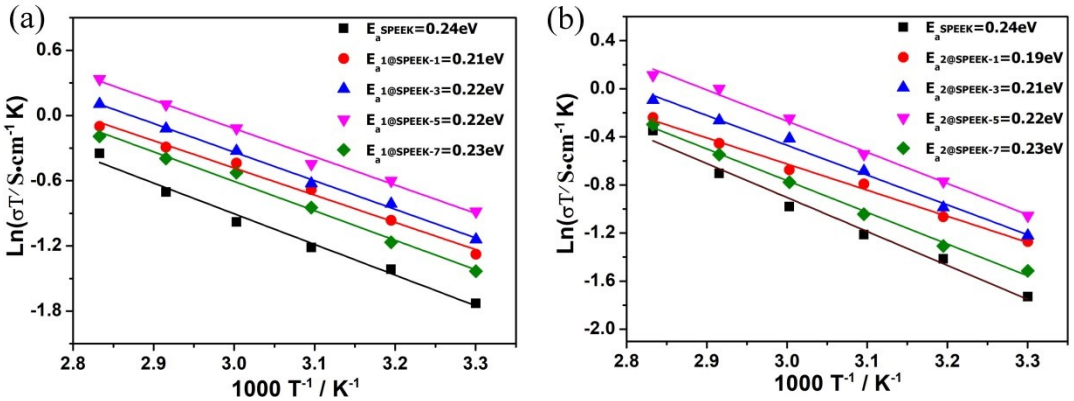

Figure S5 (a) Arrhenius plots for activation energy of pure SPEEK membrane and **1**@SPEEK-X under 98%RH; (b) Arrhenius plots for activation energy of pure SPEEK membrane and **2**@SPEEK-X under 98% RH.

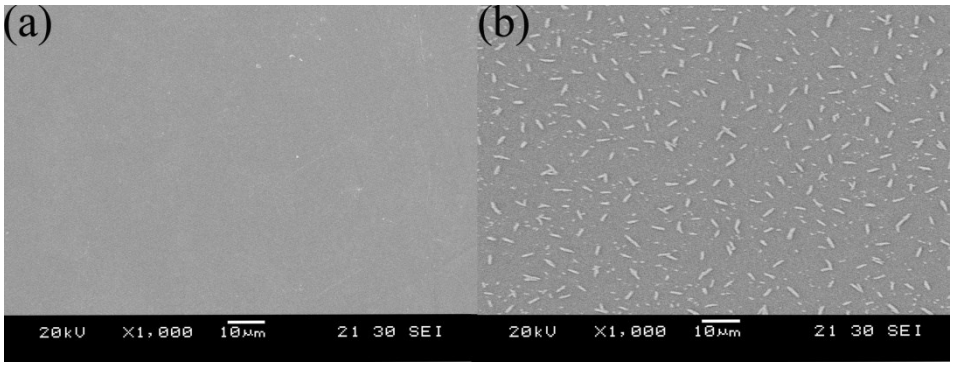

Figure S6 Surface SEM images of (a) pure SPEEK membrane and (b) **2**@SPEEK-5

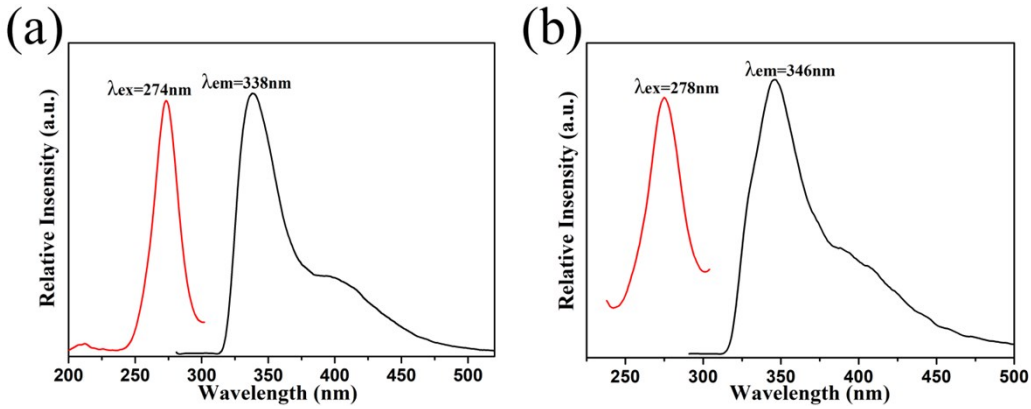

Figure S7 The excitation and emission spectra of solid state fluorescence of (a) complex **1**, and (b) complex **2.**

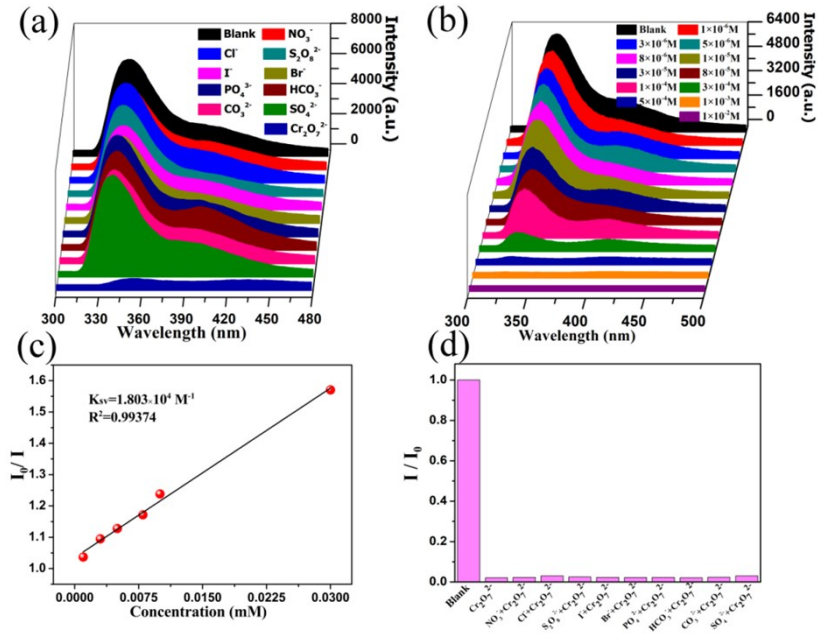

Figure S8 Emission spectra of (a) complex **2** in different anion solutions; (b) complex **2** with different concentrations of $Cr_2O_7^{2-}$ ions; (c) The Stern–Volmer plot of I_0/I versus the concentration of $Cr_2O_7^{2-}$ ions for complex **2** at low concentration (from 0 to 3×10^{-5} M), (d) Complex **2** detected $Cr_2O_7^{2-}$ ions in the presence of other anion solutions.

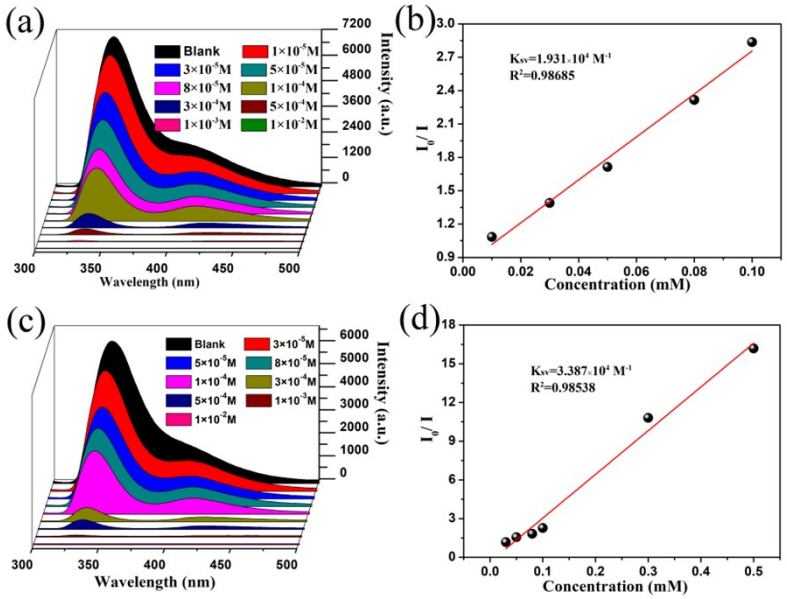

Figure S9 Emission spectra of (a) complex **1** with different concentrations of CrO_4^{2-} ions; (b) The Stern–Volmer plot of I_0/I versus the concentration of CrO_4^{2-} ions for complex **1** at low concentration (from 0 to 1×10^{-4} M), (c) complex **2** with different concentrations of CrO_4^{2-} ions; (b) The Stern–Volmer plot of I_0/I versus the concentration of CrO_4^{2-} ions for complex **2** at low concentration (from 0 to 5×10^{-4} M)

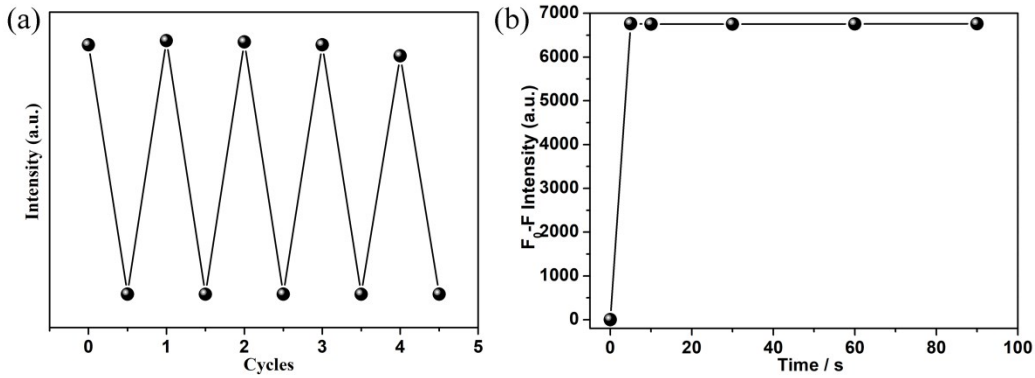

Figure S10 (a) The fluorescence reversibility study of complex **1** within 5 cycles; (b) Time-dependent response of complex **1** for $Cr_2O_7^{2-}$ (C=1×10^{-3}M)

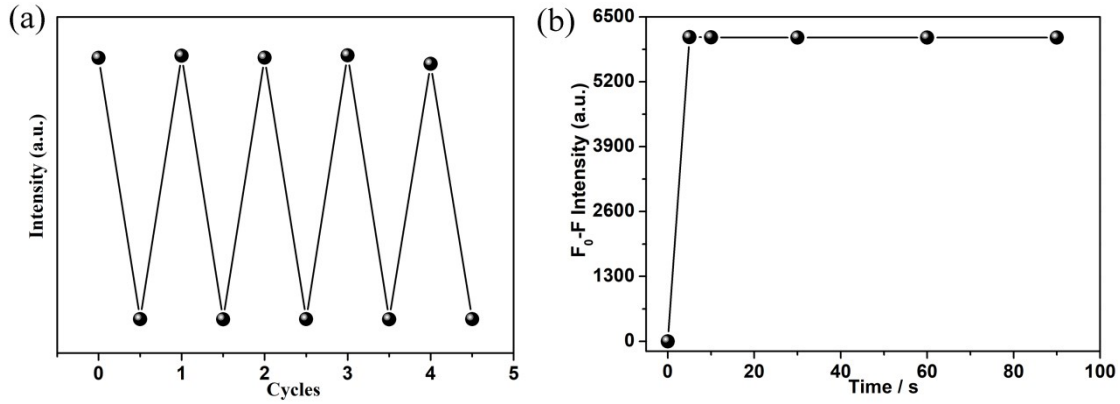

Figure S11 (a) The fluorescence reversibility study of complex **2** within 5 cycles; (b) Time-dependent response of complex **2** for $Cr_2O_7^{2-}$ ($C=1\times10^{-3}M$)

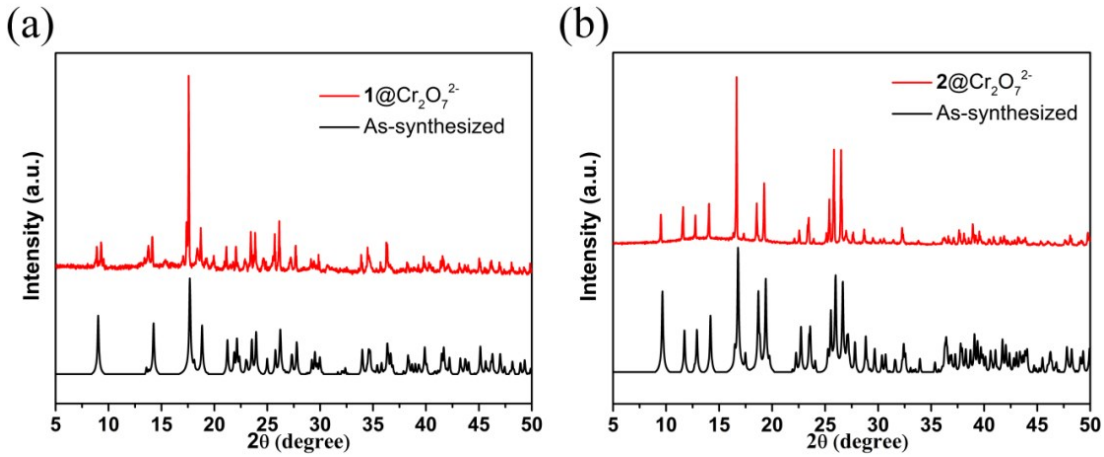

Figure S12 (a) The PXRD patterns of complex **1** after soaking in $Cr_2O_7^{2-}$ aqueous solution. (b) The PXRD patterns of complex **2** after soaking in $Cr_2O_7^{2-}$ aqueous solution.

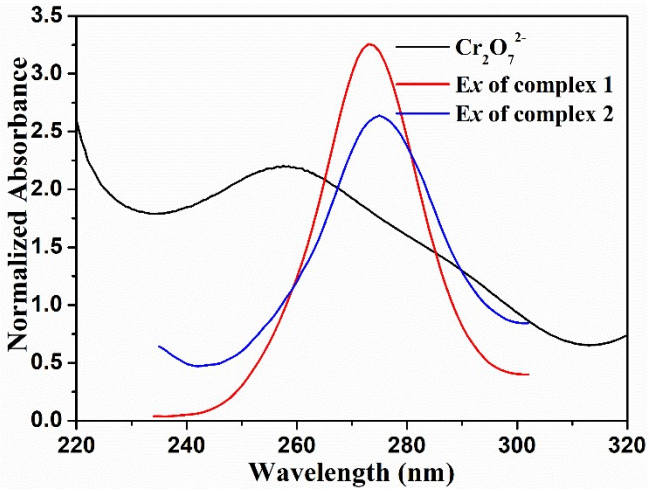

Figure S13 The excitation spectra of complex **1**, complex **2** and UV-vis absorption spectrum of $Cr_2O_7^{2-}$ ions.

Table S1 The hydrogen bonds in complex **1**

Donor---H···Acceptor	D-H	H···A	D···A	D-H···A
O(5)-H(5A)···O(2)	0.86	1.79	2.645	178
O(6)-H(6A)···O(5)	0.86	1.89	2.748	178
O(6)-H(6B)···O(3)	0.86	1.94	2.781	168
O(7)-H(7A)···O(8)	0.86	2.18	2.947	149
O(7)-H(7B)···O(3)	0.86	1.98	2.790	157
O(7)-H(7B)···O(4)	0.86	2.46	3.103	132
O(8)-H(8A)···O(1)	0.86	1.89	2.791	161
O(8)-H(8B)···O(4)	0.85	2.08	2.870	154

Table S2 The hydrogen bonds in complex **2**

Donor---H···Acceptor	D-H	H···A	D···A	D-H···A
O(5)-H(5A)···O(2)	0.82	1.83	2.646	176
O(6)-H(6A)···O(1)	0.85	1.84	2.642	158
O(6)-H(6B)···O(3)	0.85	1.83	2.655	162
O(7)-H(7A)···O(6)	0.85	1.95	2.794	174
O(7)-H(7B)···O(8)	0.85	2.28	2.966	138
O(7)-H(7B)···O(4)	0.85	2.49	3.227	145
O(8)-H(8A)···O(3)	0.85	1.83	2.677	172
O(8)-H(8B)···O(5)	0.85	1.86	2.710	177

Table S3 The proton conduction of reported complexes in the literature

Complexes	condition	Proton conductivity ($S \cdot cm^{-1}$)	Ref.
$[Cd(5\text{-hip})(H_2O)_3]_n$	98% RH, 343K	1.53×10^{-3}	This work
$[Zn(5\text{-hip})(H_2O)_3]_n$	98% RH, 353K	5.27×10^{-4}	This work
HNU-38	98% RH, 353K	1.45×10^{-3}	1
MOF-808	99% RH, 315K	7.58×10^{-3}	2
VNU-23	90% RH, 343K	1.54×10^{-4}	3
$Zr_6O_4(OH)_6(p\text{-BDC})_{5.2}$	95% RH, 338K	2.63×10^{-4}	4
$Zr_6O_4(OH)_6(p\text{-BDC})_5$	95% RH, 338K	6.93×10^{-3}	4
MOF-801	98% RH, 298K	1.88×10^{-3}	5
$[Zn(L)Cl]_n$	98% RH, 398K	4.72×10^{-3}	6
FJU-80	98% RH, 353K	1.05×10^{-3}	7
FJU-81	98% RH, 353K	4.53×10^{-3}	7

Table S4 The proton conductivity, E_a, water uptake and area swelling of composite membrane

Membrane	Proton conductivity ($S \cdot cm^{-1}$)	E_a (eV)	Water uptake (%)	Area swelling (%)
SPEEK	2.00×10^{-3}	0.24	37.71	30.21
1@SPEEK-1	2.56×10^{-3}	0.21	31.72	25.88
1@SPEEK-3	3.14×10^{-3}	0.22	27.45	23.44
1@SPEEK-5	3.95×10^{-3}	0.22	24.87	16.3
1@SPEEK-7	2.34×10^{-3}	0.23	20.63	14.23
2@SPEEK-1	2.23×10^{-3}	0.19	30.75	24.51
2@SPEEK-3	2.58×10^{-3}	0.21	26.57	18.21
2@SPEEK-5	3.17×10^{-3}	0.22	20.02	13.25
2@SPEEK-7	2.11×10^{-3}	0.23	17.2	11.89

Table S5 The performance of reported complexes for detecting $Cr_2O_7^{2-}$ in H_2O

Complexes	K_{sv} (M^{-1})	LOD (μM)	Ref.
$[Cd(5\text{-}hip)(H_2O)_3]_n$	1.15×10^4	0.8	This work
$[Zn(5\text{-}hip)(H_2O)_3]_n$	1.80×10^4	1	This work
BUT-28	1.02×10^5	0.12	[8]
BUT-39	1.57×10^4	1.5	[9]
NU-1000	1.34×10^4	1.8	[10]
$[Ag(btx)_{0.5}(DCTP)_{0.5}]_n$	1.92×10^4	2.04	[11]
$[Cd_3(cpota)_2(phen)_3]_n \cdot 5nH_2O$	1.21×10^3	0.37	[12]
$[Eu_2(tpbpc)_4 \cdot CO_3 \cdot H_2O] \cdot DMF \cdot solven$	1.04×10^4	0.33	[13]
$[Cd(IPA)(3\text{-}PN)]_n$	2.91×10^3	12.02	[14]
$[Zn(ttz)H_2O]_n$	2.19×10^3	2	[15]
$[Zn(btz)]_n$	4.23×10^3	2	[15]
$[Y(BTC)(DMF)_6]_n$:0.1Eu	4.52×10^3	0.04	[16]

REFERENCE

1. Wang, F. X.; Ren, G. J.; Tian, R. J.; Pan, Q. H., Pillared-layer MOF Based on Template-directed Method Synthesis, Structureand Proton Conduction Properties. *Chinese J. Struct. Chem.* **2020,** *39* (7), 1337-1342.
2. Luo, H. B.; Wang, M.; Liu, S. X.; Xue, C.; Tian, Z. F.; Zou, Y.; Ren, X. M., Proton Conductance of a Superior Water-Stable Metal-Organic Framework and Its Composite Membrane with Poly(vinylidene fluoride). *Inorg. Chem.* **2017,** *56* (7), 4169-4175.
3. Nguyen, M. V.; Lo, T. H. N.; Luu, L. C.; Nguyen, H. T. T.; Tu, T. N., Enhancing proton conductivity in a metal–organic framework at T > 80 °C by an anchoring strategy. *Journal of Mater. Chem. A* **2018,** *6* (4), 1816-1821.
4. Taylor, J. M.; Dekura, S.; Ikeda, R.; Kitagawa, H., Defect Control To Enhance Proton Conductivity in a Metal–Organic Framework. *Chem. Mater.* **2015,** *27* (7), 2286-2289.
5. Zhang, J.; Bai, H. J.; Ren, Q.; Luo, H. B.; Ren, X. M.; Tian, Z. F.; Lu, S., Extra Water- and Acid-Stable MOF-801 with High Proton Conductivity and Its Composite Membrane for Proton-Exchange Membrane. *ACS Appl. Mater. Interfaces* **2018,** *10* (34), 28656-28663.
6. Shi, Z. Q.; Ji, N. N.; Wang, M. H.; Li, G., A Comparative Study of Proton Conduction Between a 2D Zinc(II) MOF and Its Corresponding Organic Ligand. *Inorg. Chem.* **2020,** *59* (7), 4781-4789.
7. Que, Z.; Ye, Y.; Yang, Y.; Xiang, F.; Chen, S.; Huang, J.; Li, Y.; Liu, C.; Xiang, S.; Zhang, Z., Solvent-Assisted Modification to Enhance Proton Conductivity and Water Stability in Metal Phosphonates. *Inorg. Chem.* **2020,** *59* (6), 3518-3522.
8. Xu, M. M.; Kong, X. J.; He, T.; Wu, X. Q.; Xie, L. H.; Li, J. R., A Stable Zr(IV)-Based Metal-Organic Framework Constructed from C horizontal lineC Bridged Di-isophthalate Ligand for Sensitive Detection of Cr2O7(2-) in Water. *Inorg Chem* **2018,** *57* (22), 14260-14268.
9. He, T.; Zhang, Y. Z.; Kong, X. J.; Yu, J.; Lv, X. L.; Wu, Y.; Guo, Z. J.; Li, J. R., Zr(IV)-Based Metal-Organic Framework with T-Shaped Ligand: Unique Structure, High Stability, Selective Detection, and Rapid Adsorption of Cr2O7(2-) in Water. *ACS Appl Mater Interfaces* **2018,** *10* (19), 16650-16659.
10. Lin, Z. J.; Zheng, H. Q.; Zheng, H. Y.; Lin, L. P.; Xin, Q.; Cao, R., Efficient Capture and Effective Sensing of Cr2O7(2-) from Water Using a Zirconium Metal-Organic Framework. *Inorg. Chem.* **2017,** *56* (22), 14178-14188.
11. Chang, H.-N.; Liu, L.-W.; Hao, Z. C.; Cui, G.-H., A 3D Ag(I) metal-organic framework for sensing luminescence and photocatalytic activities. *Journal of Molecular Structure* **2018,** *1155*, 496-502.
12. Li, S.; Lu, L.; Zhu, M.; Yuan, C.; Feng, S., A bifunctional chemosensor for detection of volatile ketone or hexavalent chromate anions in aqueous solution based on a Cd(II) metal–organic framework. *Sensors and Actuators B: Chemical* **2018,** *258*, 970-980.
13. Liu, J.; Ji, G.; Xiao, J.; Liu, Z., Ultrastable 1D Europium Complex for

Simultaneous and Quantitative Sensing of Cr(III) and Cr(VI) Ions in Aqueous Solution with High Selectivity and Sensitivity. *Inorg. Chem.* **2017,** *56* (7), 4197-4205.
14. Parmar, B.; Rachuri, Y.; Bisht, K. K.; Laiya, R.; Suresh, E., Mechanochemical and Conventional Synthesis of Zn(II)/Cd(II) Luminescent Coordination Polymers: Dual Sensing Probe for Selective Detection of Chromate Anions and TNP in Aqueous Phase. *Inorg. Chem.* **2017,** *56* (5), 2627-2638.
15. Cao, C.-S.; Hu, H.-C.; Xu, H.; Qiao, W.-Z.; Zhao, B., Two solvent-stable MOFs as a recyclable luminescent probe for detecting dichromate or chromate anions. *CrystEngComm* **2016,** *18* (23), 4445-4451.
16. Duan, T.-W.; Yan, B.; Weng, H., Europium activated yttrium hybrid microporous system for luminescent sensing toxic anion of Cr(VI) species. *Microporous and Mesoporous Materials* **2015,** *217*, 196-202.